Journal of Energy, Environmental & Chemical Engineering
2024; Vol. 9, No. 1, pp. 33-45
https://doi.org/10.11648/j.jeece.20240901.14

Research Article

Mathematical Prediction of Electrical Solar Energy Based on Solar Data for Two Main Cities of Chad: Mongo in the Centre and Pala in the South of Chad

Ali Ramadan Ali[1], Mahamat Kher Nediguina[2], Adoum Kriga[1], Marinette Jeutho Gouajio[3], Adoum Danao Adile[1], Fabien Kenmogne[4, *], Abakar Mahamat Tahir[1]

[1]Department of Industrial Engineering and Maintenance, Polytechnic University of Mongo, Mongo, Chad

[2]Department of Physics, Faculty of Exact and Applied Sciences, University of Ndjamena (Scientific Facilitator in Cecoqda), Ndjamena, Chad

[3]Department of Fundamental and Transversal Sciences, National Advanced School of Public Works, Yaoundé, Cameroon

[4]Department of Civil Engineering, Advanced Teacher Training College of the Technical Education, University of Douala, Douala, Cameroon

Abstract

The comparative study of the solar powers between two main cities of Chad is performed in the present work, the city of Mongo in the Centre and that of Pala in the South, with an aim of knowing which one of the two cities is more adequate for an installation of the solar power station, taking into account the regional climatic and environmental conditions of both cities. To do this, the graphical statistical analysis of long-term solar irradiance data and temperature is performed. The data used is that of the decade (2010-2020), based on solar radiation data handed by the National Aeronautics and Space Administration (NASA) and Photovoltaic Geographical Information System (PGIS) for Mongo in the centre and Pala in the south of Chad. The shape of the mean monthly irradiation has been plotted and has been approximated using the sinusoidal function through the mean square analysis. The temperature data has been also obtained by the same process and plotted versus irradiance in order to find the adequate mathematical relationship between them. For the statistical analysis, the maximum entropy principle has been used. As results, it is found that the maximum irradiance is obtained in March, which are 226.26kWh/m^2 for Pala and 219.355kWh/m^2 for Mongo, while the minimum irradiances are obtained in August, which are 151.67kWh/m^2 for Pala and 158.9kWh/m^2 for Mongo. The temperature data is also obtained and the mean monthly data plotted, showing that apart for the months of March and April, the the shapes of irradiation and temperatures are similar for both sites. Then it is found that the frequency and probability density distributions reach their maximum at the same dates.

Keywords

Irradiation Solar Data, Temperature Data, Maximum Entropy Principle, Mean Square Analysis, Statistical Analysis

*Corresponding author: cabenset@yahoo.fr (Fabien Kenmogne)

Received: 6 February 2024; **Accepted:** 26 February 2024; **Published:** 13 March 2024

1. Introduction

Because of the rampant of desertification in Chad combined with widespread awareness, encourages the population and the government to opt for the development of renewable energies, solar and wind [1]. In 2008, faced with desertification which threatens the entire country, the Chadian government banned the use of firewood and charcoal, the main energy sources for Chadian households [2]. The majority of them have spent difficult months with a National Electricity Company which is struggling to regularly supply energy and faced with the high cost and scarcity of butane gas, imposed as a substitute fuel [3]. It is under these conditions that the promotion of renewable energies, particularly the sun and the wind, find their importance as a source of substitution for exhaustible and polluting conventional energies [4]. Every day, one receives about a thousand times more solar energy than that needed. The sun is so strong, and this energy source is renewable, clean and safe. For everyday household use, for example, using a solar oven saves money compared to bundles or gas [5].

The actors thus involved in the field of energy the support of the government intend to popularize the production of appropriate and adapted solar electricity, promote self-employment and reduce the consumption of energy sources, fossil fuels [6]. For the moment, electrical energy still remains a big problem for households and businesses in Chad [7]. Designing a renewable electricity generation system requires knowledge of the optimal power generated by existing resources (sun and wind), and knowledge of the optimal power requested by households (electrical load) [8]. This is why it is necessary to analyze in depth the optimal minimum powers generated by the sun or the wind, depending on the cities chosen.

It should be noted that Chad, which is a country in Sahelian Africa, has significant potential, such as wind, solar and biomass. From north to south of Chad, the sun shines 2,750 to 3,250 hours per year; which gives on average 4 to 6 kilowatts/hour per square meter per day [9]. During the period from March to May, the temperature can vary from 35 ℃ to 40 ℃ in the shade, or even more, in Mongo in central Chad. As for wind power, it appears that Chad has a very significant deposit in the northern regions and moderately in the central areas, where there are mountain ranges. But all these renewable energy resources, although abundant, don't appear in Chad's energy balance sheet mainly due to their low level of exploitation:

The main objective of the present work is to deeply investigate the possibility to supply two main cities of Chad with solar energy, Mongo in the Centre and Pala in the South by using statistical method, which is usually used for wind energy, but which is new in the context of solar energy.

2. Materials and Methods

2.1. Irradiance Solar Data

The Irradiance solar data used in this paper were obtained from NASA meteorological services (2010-2020) and PGIS for Pala and Mongo. Pala site is the city located in the south of Chad, while Mongo is the city located in the center of Chad. They are framed by the geographical coordinates presented in Table 1, while the irradiance data found are summarized in the tables of the appendixes.

Table 1. *Geographical coordinates of the studied sites.*

Site	North Latitude	East Longitude	Elevation
Mongo	9.36˚	14.9˚	388.8m
Pala	12.23˚	18.82˚	495.79 m

2.2. Sinusoidal Curve Approximation by the Mean Square Analysis

In the present paper, according to the profile of curve that will be obtained, the irradiance will be approximated using the following sinusoidal function:

$$P(t_i) = a + bcos(t_i) + csin(t_i) \quad (1)$$

Where $t_i = [1,2,\ldots,12]$ is associated to the corresponding month from January to December, and where the parameters a, b and c will be determined by minimizing the error

$$\Delta P^2 = \sum_{n=1}^{N}(P_i - P(t_i))^2 \quad (2)$$

as follows $\frac{\partial}{\partial a}(\Delta P^2) = 0$; $\frac{\partial}{\partial b}(\Delta P^2) = 0$; and $\frac{\partial}{\partial c}(\Delta P^2) = 0$, leading to the following equation:$AX = B$, with

$$A = \begin{bmatrix} N & \sum_{n=1}^{N}\cos(t_i) & \sum_{n=1}^{N}\sin(t_i) \\ \sum_{n=1}^{N}\cos(t_i) & \sum_{n=1}^{N}\cos^2(t_i) & \frac{1}{2}\sum_{n=1}^{N}\sin(2t_i) \\ \sum_{n=1}^{N}\sin(t_i) & \frac{1}{2}\sum_{n=1}^{N}\sin(2t_i) & N - \sum_{n=1}^{N}\cos^2(t_i) \end{bmatrix}, \; B = \begin{bmatrix} \sum_{n=1}^{N}P_i \\ \sum_{n=1}^{N}P_i\cos(t_i) \\ \sum_{n=1}^{N}P_i\sin(t_i) \end{bmatrix}, \; X = \begin{bmatrix} a \\ b \\ c \end{bmatrix}, \quad (3)$$

which will be solved as X=B/A in MATLAB software.

2.3. Statistical Analysis Using the Maximum Entropy Principle

In order to study the maximum entropy principle, the probability density function of speed has been introduced in the following form:

$$f(P) = \exp\left(\sum_{j=1}^{M} \alpha_j P^j\right) = \exp(\alpha_0 + \alpha_1 P + \alpha_2 P^2 + \alpha_3 P^3 + \cdots), \quad (4)$$

where α_j are the Lagrangian multipliers, while M is the number of the low order moments used, and where P is the irradiance distribution. This density function is obtained by minimizing the Shannon's entropy, following the well-known Carla et al principles [10-14], suggesting the following constraints:

$$\int_0^{\max(v)} f(P)d(P) = 1, \int_0^{\max(v)} Pf(P)d(P) = m_i' \quad (5)$$

$m_{i'}$, being the m-low statistical orders, obtained empirically as [15]

$$m_i' = \frac{1}{N}\sum_{i=1}^{N} P^i. \quad (6)$$

The set of equations 5 and 6 will be solved using the Matrix Laboratory (MATLLAB) software.

2.4. Estimation of Extraterrestrial Radiation, *H0*

The monthly mean of the daily extraterrestrial solar radiation on a horizontal surface is determined according the following relation [16-20]:

$$H_0 = \frac{24}{\pi} I_{sc}\left[1 + 0.33\cos\left(\frac{360D_n}{365}\right)\right] \times \left[\cos L \cos\delta \sin\omega_s + \frac{2\pi\omega_s}{360}\sin L \sin\delta\right]. \quad (7)$$

δ and ω_s being respectively the monthly mean of the daily solar declination and the sunshine hour angle defined by [21-23]:

$$\delta = 23.45\sin\left(\frac{360(284+D_n)}{365}\right), \omega_s = \cos^{-1}(-\tan L \tan\delta). \quad (8)$$

In Eq. (4) I_{sc} is the solar constant ($I_{sc} = 1367\ W/m^2$), L is the location latitude, D_n is the number of the day in the year.

3. Results and Discussion

3.1. Analysis of Monthly Irradiation of Both Sites

Figures 1 and 2 (a and b) show plots of the irradiance for the horizontal plane (a) and inclined plane (b), of Mongo and Pala, respectively, from 2010 to 2020. As one can see, they have nearly the same shape close to sinusoidal one, justifying then the approximation using Eq.(1).

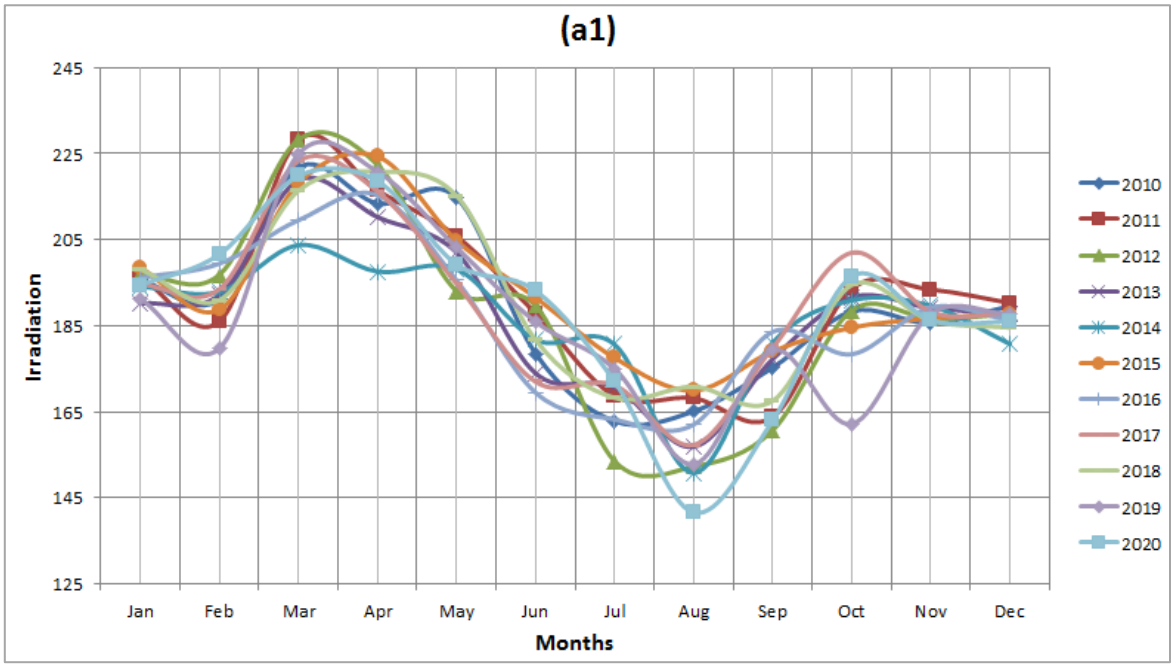

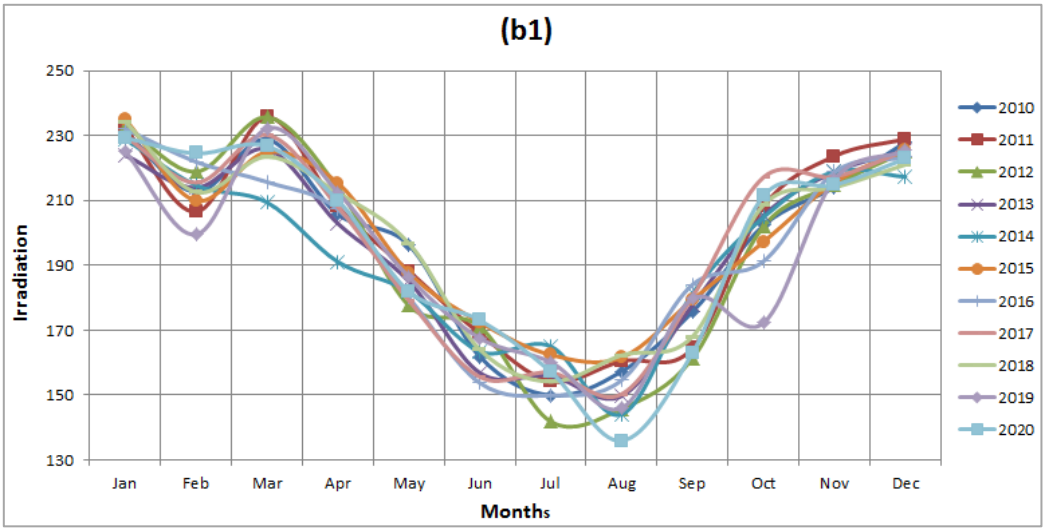

Figure 1. *Yearly Irradiation of Mongo in* (kWh/m^2)*, (a): on the horizontal plane. (b): on the inclined plane.*

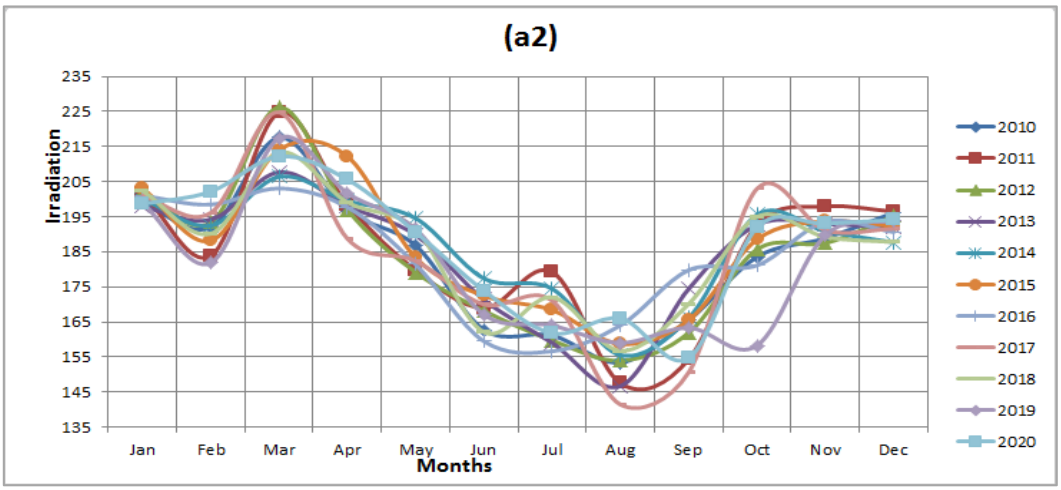

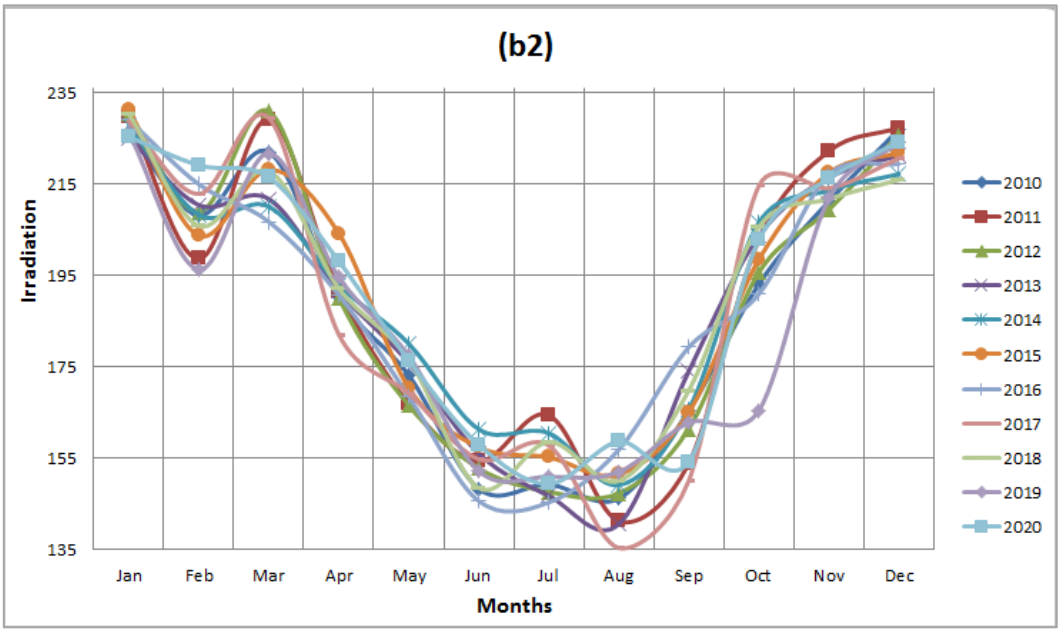

Figure 2. *Yearly Irradiation of Pala in* (kWh/m^2) *(a): on the horizontal plane. (b): on the inclined plane.*

In order to make the comparative study of the irradiation of both sites, Mongo and Pala, the mean values of irradiance over 11 years from 20120 to 2020 are calculated and summarized in Table 2, allowing drawing graphs of Figures 3 (a) for the horizontal plane, and (b) for the inclined plane. In Figure 2a, the irradiance in the horizontal plane of Pala is greater than that of Mongo from January to February, and From October to December. Otherwise the irradiance of Mongo is greater than that of Pala. While for the inclined plane, as shown in Figure 2b, the irradiation of Mongo is always greater than that of Pala. The maximum irradiance is obtained in March, which are 226.26 kWh/m^2 for Pala and 219.355 kWh/m^2 for Mongo, while the minimum irradiance is obtained in August, which are 151.677 kWh/m^2 for Pala and 158.9 kWh/m^2 for Mongo. Which are understandable 'since in August, it is raining in the entire of Chadian country. This result could help engineers, in the construction of the photovoltaic cells for electric energy supply.

Table 2. *Mean Monthly irradiation (kWh/m^2), (A): on the horizontal plane, (B): on the inclined plane. (A1 and B1): Mongo, (A2 and B2): Pala.*

	Jan	Feb	Mar	Apr	May	Jun	July	Aug	Sept	Oct	Nov	Dec
A1	195.12	192.01	219.355	216	202.40	182.31	169.41	158.9	173.73	188.28	188.08	186.92
B1	230.46	213.71	226.26	207.93	185.55	164.44	155.28	151.677	174.16	201.9	217.02	224.41
A2	200.52	192.08	215.23	199.56	186.41	168.52	166.13	154.83	164.24	188.01	191.68	192.52
B2	228.13	207.86	219.41	192.52	172.76	153.53	153.21	148.04	163.75	198.08	214.55	222.14

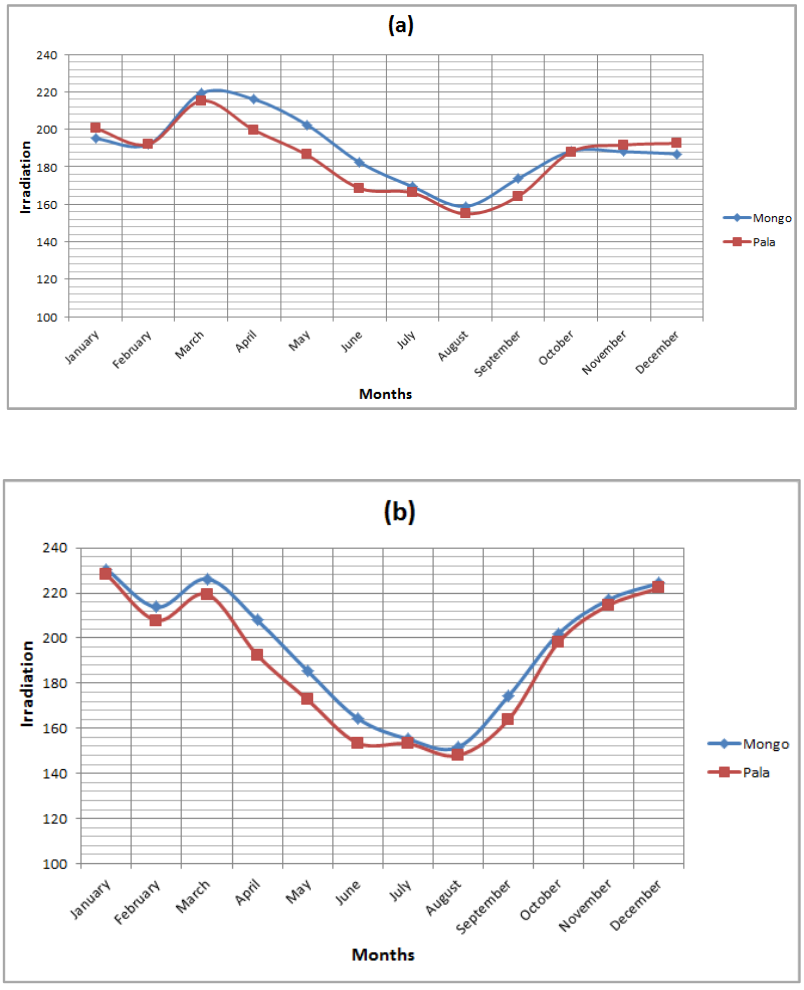

Figure 3. *Average Irradiation on the horizontal plane (kWh/m^2) of Mongo (blue) and Pala (Red). (a): on horizontal plane. (b) On inclined plane.*

By using Equation (3), it is obvious that one can approximate the irradiance on the horizontal plane of Mongo, using the following equation:

$$P(t) = 188.8788507 - 8.165273733cos(t) - 11.04633943sin(t), \quad (9)$$

while that of Pala is given by:

$$P(t) = 184.5893550 - 6.515675645cos(t) - 7.571103382sin(t). \quad (10)$$

These equations are plotted in dashed curve of Figure 5 for Mongo and Pala, respectively.

In figure 5, the solution given by Eq. (7) is plotted as well as P given in table 4, justifying that one can approximate fairly the irradiance using Equation (7).

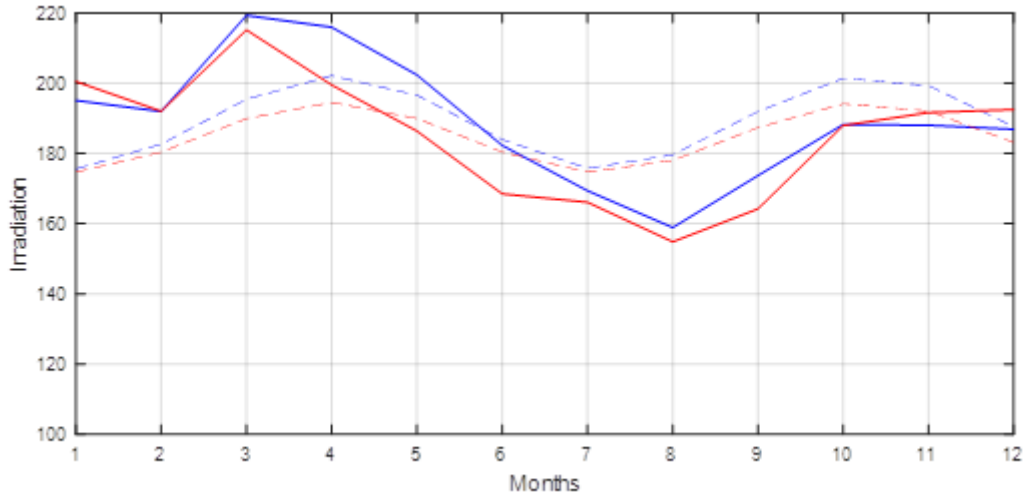

Figure 4. *Mean monthly irradiation on the horizontal plane (kWh/m^2) of Mongo (blue) and Pala (Red): Continuum: Using the data given in Table 2, Dashed: obtained using Eq. (3).*

3.2. Analysis of Temperatures for Both Sites

In order to study the relationship between temperatures and irradiation, the temperature mean monthly data have been calculated and the results is contained in Table 3, leading by plotting both the temperature versus time as shown in Figure 5 to the following remarks:

Pala has the temperature greater than that of Mongo from January to March, and from October to December, while elsewhere, Mongo has the greater temperature as compared to that of Pala. The highest temperature is obtained in April, which is on the contrary of the maximum irradiance which is found in March. The Minimum temperature is nearly obtained in August, which is in agreement with results found for irradiation on the horizontal plane.

The plot of irradiance depend of temperature as shown in Figure 6 (a and b) shows the hysteresis form, justifying the nonlinear dependency of irradiance versus the temperature.

Table 3. *Mean Monthly temperature (°C), A: Mongo, B: Pala.*

	Jan	Feb	Mar	Apr	May	Jun	July	Aug	Sept	Oct	Nov	Dec
A	24.81	27.82	31.51	33.19	32.67	29.53	26.75	24.91	25.42	26.19	25.81	24.55
B	26.22	28.897	32.55	32.95	30.23	27.97	25.68	24.70	25.29	26.1	26.91	25.99

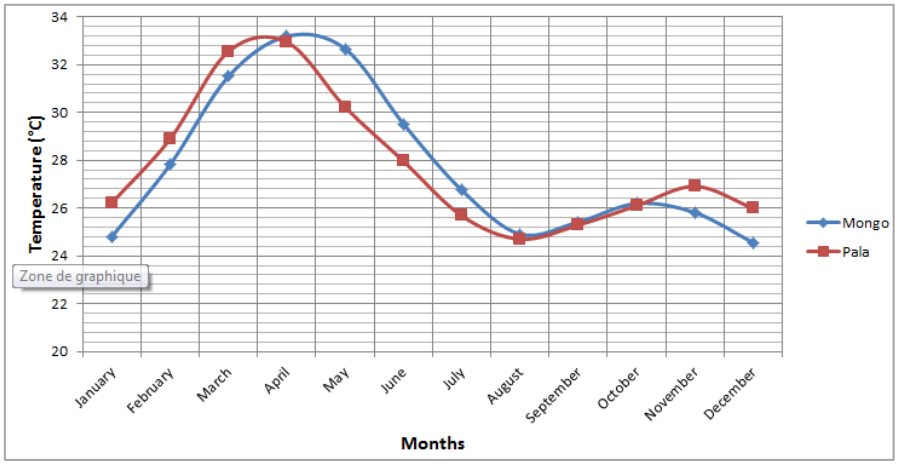

Figure 5. *Average Temperature (˚C) at 10m high.*

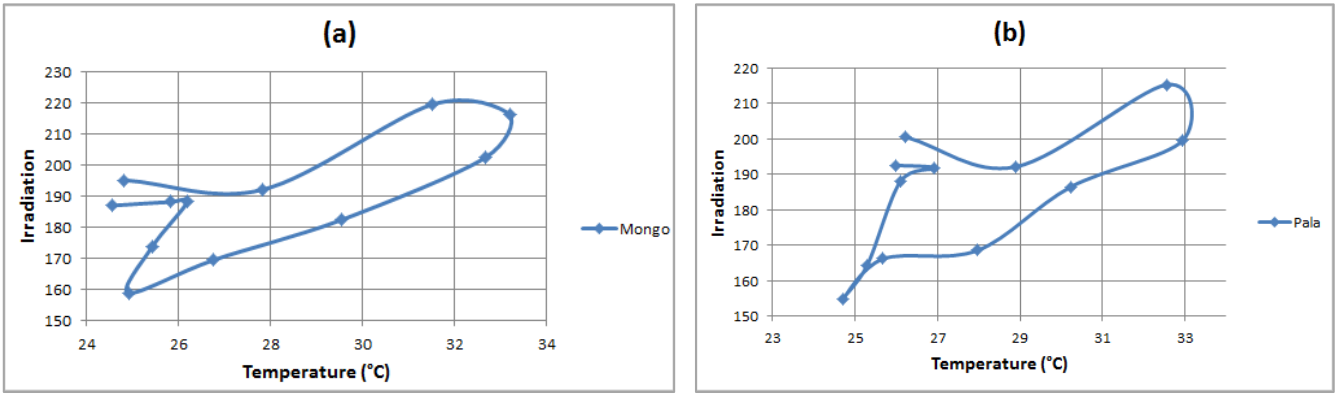

Figure 6. *Irradiation versus average temperature, showing the curve in form of hysteresiy.*

3.3. Statistical Analysis of Mongo and Pala Sites

The frequency of power distribution is given in the following tables 4 and 5 for Mongo, for horizontal plane and for the inclined plane, respectively, which allow plotting the curve of Figure 7. By the same process, the curves of Figure 8 is plotted for Pala, which lead to the fact that: For Mongo, the maximum frequency on the horizontal plane is found for the irradiation of 185 kWh/m^2, while for Pala, the maximum is for 190 kWh/m^2. In these figures, the probability density distribution, calculated following the maximum entropy principle outlined in Eqs. (4, 5, 6) is plotted as appeared in blue color, from where it is seen that both the frequency and probability density distribution have the same shape. The distribution is normal for the horizontal plane, while for the inclined plane, the distribution is the increasing function of the irradiation.

Table 4. *Frequency of power distribution in the horizontal plane of Mongo.*

Power	140	150	155	160	165	170	175	180	185	190	195	200	205	210	215	220	225	Total
eff	1	4	2	7	5	8	6	10	22	20	16	7	2	3	9	6	4	132

Table 5. *Frequency of power distribution in the inclined plane of Mongo.*

Power	135	140	145	150	155	160	165	170	175	180	185	190	195
eff	1	1	3	5	9	9	6	4	3	8	5	2	3

200	205	210	215	220	225	230	235	Total
4	9	11	16	7	14	8	4	132

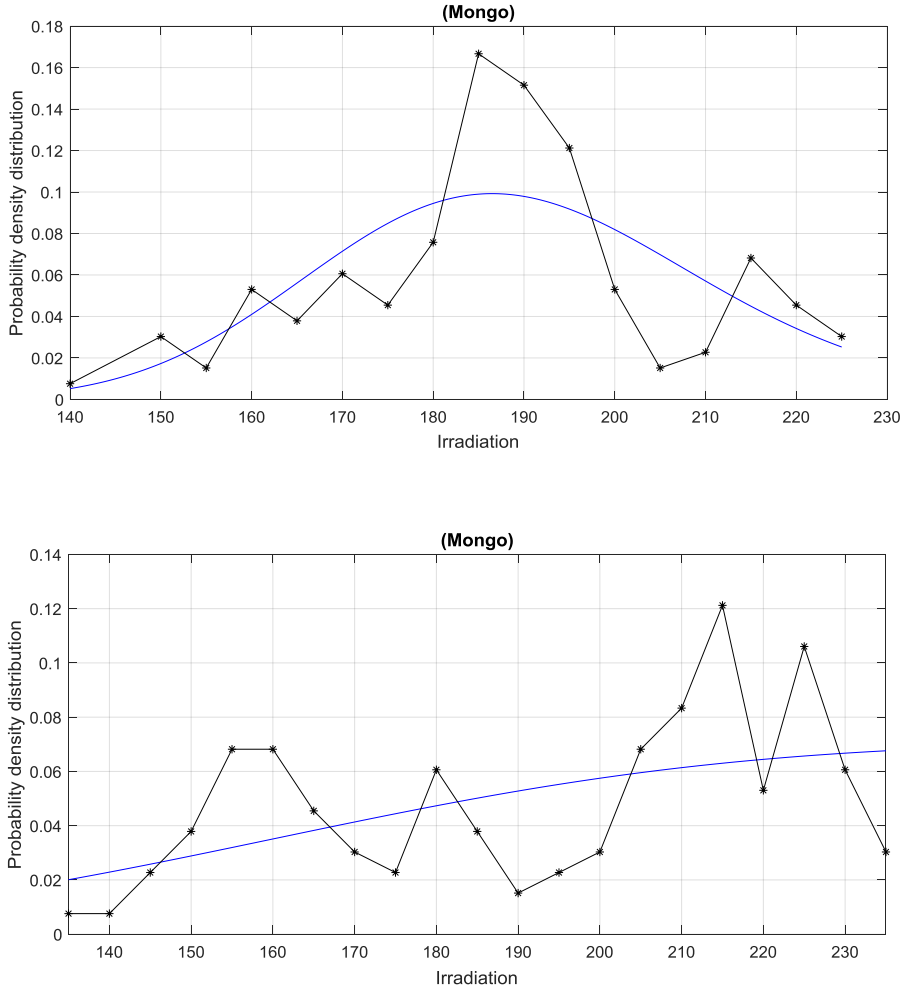

Figure 7. *Probability distribution over ten years for the city of Mongo and for the (black): the frequency given in Tables 4 and 5. (blue): the probability given by Eq.(6), with (top): horizontal plane for* $\alpha = [74.9438, -0.9591, 0.00402, -5.1802 \times 10^{-6}]$. *(bottom) inclined plane with* $\alpha = [1.00, 194.5833333, 38651.70455, 7.81997822 \times 10^{6}]$.

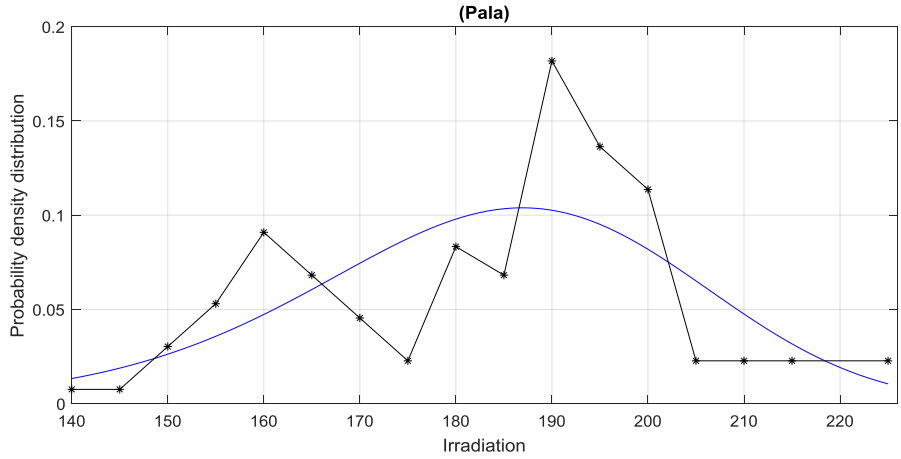

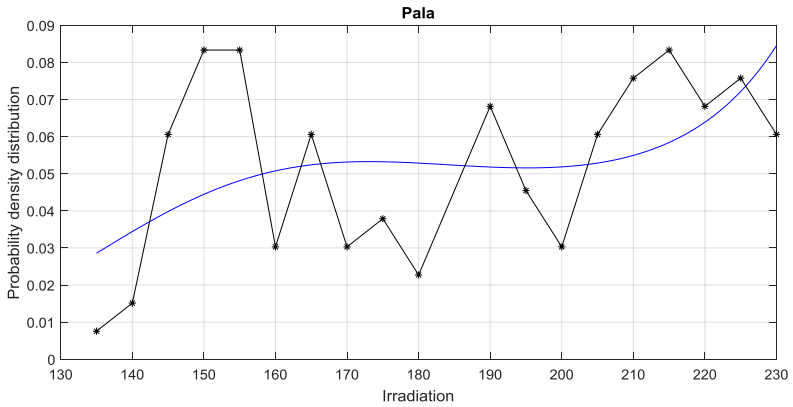

Figure 8. *Probability distribution over ten years for the city of Pala and for: (black): the frequency given in Table 5. (blue): the probability given by Eq.(6), with (left): horizontal plane for* $\alpha = [-2.4877939, 0.31758, -0.00299, 7.63417 \times 10^{-6}]$. *(right) inclined plane with* $\alpha = [40.060264, -0.6089, 0.003318, -6.006319 \times 10^{-6}]$.

4. Conclusion

The electrical solar energy has been evaluated for two main cities of Chad, that is Mongo in the centre and Pala in the south based on solar data obtained from the NASA and PGIS for the period going to 2010 to 2020. As methodology, the graphical statistical analysis of long-term solar irradiance data and temperature is performed. Then the shape of the mean monthly irradiation has been plotted and has been approximated using the sinusoidal function by using the mean square analysis. The temperature data has been also obtained and plotted versus irradiance in order to find the adequate mathematical relationship between them. For the statistical analysis, the maximum entropy principle has been used. As results, it is found that the maximum irradiance is obtained in March, which are 226.26 kWh/m^2 for Pala and 219.355 kWh/m^2 for Mongo, while the minimum irradiances are obtained in August, which are 151.67 kWh/m^2 for Pala and 158.9 kWh/m^2 for Mongo. These results are understandable 'since in August, it is raining in the entire of Chadian country. The dependency of temperature with irradiation is the hysteresis form, justifying that their dependency is a nonlinear function. Apart for the months of March and April, both the shapes of irradiation and temperatures are similar for both sites. It is also found that the frequency and probability density distributions reach their maximum at the same dates, which are 1859 kWh/m^2 for Mongo and 190 9 kWh/m^2 for Pala. The present analysis could then help engineers and designers in evaluating of photovoltaic cell powers for the supplying in solar energy in both cities.

It is important to note that the curves obtained for the frequencies are not smooth, which are why the probability doesn't fit all the points obtained for the frequencies. This may be due to the fact that the data are monthly, and therefore very few points obtained. It would be very important to carry out the work of this paper using hourly or daily data, which would surely give better results. Work in this direction will constitute perspectives for future work.

Abbreviations

NASA: National Aeronautics and Space Administration
PGIS: Photovoltaic Geographical Information System
MATLLAB: Matrix Laboratory

Conflicts of Interest

The authors declare no conflicts of interest.

Appendix

Irradiance and temperature data of the cities of Mongo and Pala

Table 6. *Yearly irradiation on the horizontal plane* (kWh/m^2) *for Mongo.*

year	Jan	Feb	Mar	Apr	May	Jun	Jul	Aug	Sep	Oct	Nov	Dec
2010	195.61	191.12	221.79	213.41	214.77	178.51	162.81	165.13	175.3	188.32	185.59	189.59
2011	196.35	186.02	228.25	216.41	205.75	187.84	168.67	168.19	163.84	193.58	193.39	190.3

year	Jan	Feb	Mar	Apr	May	Jun	Jul	Aug	Sep	Oct	Nov	Dec
2012	196.91	196.86	228.24	222.37	193.08	189.65	153.49	152.26	160.76	188.57	186.69	187.66
2013	190.16	192.19	218.8	210.23	201.99	173.93	170.76	156.88	177.29	191.57	189.13	187.68
2014	194.1	192.87	203.74	197.57	198.18	181.74	180.63	150.81	181.13	190.93	189.62	180.75
2015	198.48	188.76	218.13	224.32	204.76	191.57	177.51	169.94	179.09	184.59	186.71	187.83
2016	196.17	199.44	209.52	215.35	195.53	169.46	163.2	162.04	183.61	178.39	189.3	186.27
2017	194.68	193.53	223.29	216.19	194.75	171.99	171.17	157.33	179.95	202	188.21	187.85
2018	198.13	190.97	216.41	220.77	215.18	181.66	168.23	170.87	167.58	194.48	186.2	184.56
2019	191.28	179.74	224.94	220.78	203.18	185.9	175	152.8	179.4	162.18	187.78	187.68
2020	194.43	201.59	219.8	218.6	199.24	193.14	172.02	141.62	163.04	196.46	186.29	185.93

Table 7. *Yearly optimal irradiation on the inclined plane (kWh/m^2) for Mongo.*

year	Jan	Feb	Mar	Apr	May	Jun	Jul	Aug	Sep	Oct	Nov	Dec
2010	231.12	212.63	228.85	205.75	196.26	161.88	149.95	157.31	175.72	202.35	214.08	227.94
2011	232.27	206.52	235.7	208.14	188.25	168.96	154.28	160.51	164.45	208.06	223.67	228.99
2012	232.98	218.88	235.68	213.88	177.59	171.12	141.87	145.87	161.36	202.07	214.85	225.15
2013	223.99	213.98	225.83	202.87	185.08	156.87	156.01	149.75	177.83	205.43	218.79	225.41
2014	228.99	214.69	209.43	191.07	181.86	163.46	165.04	144.11	181.43	204.88	218.93	217.3
2015	235.03	209.95	224.93	215.35	187.66	172.43	162.45	161.61	179.44	197.24	215.55	225.63
2016	232.13	221.91	215.7	207.25	180.13	153.76	149.92	154.63	184.11	191.27	218.78	223.32
2017	229.75	215.56	230.23	208.04	179.18	155.62	156.99	150.34	180.41	217.19	217.36	225.41
2018	234.34	212.6	223.5	212.35	196.78	164.03	154.17	162.32	168.09	208.66	213.99	221.06
2019	225.14	199.54	232.27	212.45	186.33	167.54	160.19	146.04	179.77	172.27	216.44	225.38
2020	229.36	224.52	226.79	210.04	181.97	173.13	157.25	135.96	163.11	211.45	214.77	222.88

Table 8. *Yearly irradiation on the horizontal plane (kWh/m^2) for Pala.*

year	Jan	Feb	Mar	Apr	May	Jun	Jul	Aug	Sep	Oct	Nov	Dec
2010	199	192.06	217.58	196.81	186.78	162.76	161.14	153.43	165.54	183.55	188.88	196.16
2011	201.63	183.85	224.66	198.48	179.72	168.99	179.27	147.51	154.36	192.64	197.92	196.5
2012	202.21	193.34	226.22	196.98	179.16	168.17	159.73	153.98	161.9	185.69	187.47	195.21
2013	197.83	194.18	207.71	198.08	189.79	171.36	159.04	146.69	174.47	192.7	192.94	191.84
2014	199.98	192.49	206.42	199.57	194.56	177.41	174.46	155.55	166.15	195.6	190.92	187.7
2015	203.12	188.17	214.15	212.22	183.33	172.48	168.38	158.71	165.54	188.53	193.72	192.22
2016	201.05	198.47	203.1	197.74	181.4	159.49	156.65	164	179.79	181.13	193.55	190.64
2017	200.84	196.15	224.76	188.77	182.36	169.98	171.04	141.43	150.66	203.01	191.15	191.58
2018	202.41	190.16	213.34	199.12	191.38	162.09	172.01	156.78	170.16	195.01	189.24	187.8
2019	199.01	181.85	217.42	201.74	191.48	167.09	163.96	159.04	163.34	158.27	189.71	193.93

year	Jan	Feb	Mar	Apr	May	Jun	Jul	Aug	Sep	Oct	Nov	Dec
2020	198.66	202.21	212.22	205.64	190.59	173.91	161.78	166.03	154.74	191.94	193.02	194.13

Table 9. *Yearly optimal irradiation on the inclined plane (kWh/m^2) for Pala.*

year	Jan	Feb	Mar	Apr	May	Jun	Jul	Aug	Sep	Oct	Nov	Dec
2010	226.17	208.13	221.96	190.21	173.08	148.29	149.19	146.17	165.33	193.05	211.11	226.87
2011	229.71	198.58	229.1	191.61	166.85	154.38	164.38	141.19	153.85	202.79	222.09	227.24
2012	230.31	208.86	230.84	190.07	166.48	152.76	147.64	147.3	161.4	195.59	209.29	225.64
2013	225.07	210.33	211.66	191.51	175.84	155.97	146.73	140.53	174	203.58	216.3	221.2
2014	227.61	208.19	209.99	192.81	180	161.29	160.43	149.1	165.66	206.49	213.53	217.09
2015	231.27	203.64	218.06	204.13	170.33	157.35	155.17	151.42	165.02	198.41	217.32	221.76
2016	229	214.87	206.68	190.69	168.43	145.6	145.3	156.83	179.23	190.87	216.91	219.31
2017	228.62	212.77	229.37	182	169.14	154.73	157.73	135.33	150.07	214.52	213.97	220.5
2018	230.33	205.79	217.78	192.11	176.6	148.46	158.49	150.01	169.78	205.55	211.69	215.84
2019	226.14	196.23	221.64	194.52	177.34	152.13	150.93	151.95	162.75	165.35	211.76	223.88
2020	225.25	219.02	216.4	198.04	176.3	157.91	149.33	158.6	154.2	202.73	216.07	224.16

Table 10. *Temperature (˚C) at 2m above the ground of Mongo.*

year	Jan	Feb	Mar	Apr	May	Jun	Jul	Aug	Sep	Oct	Nov	Dec
2010	26.3	28.5	29.8	33	33	30.2	26.1	25.1	25.7	26.8	27.2	23.6
2011	22.6	28.1	28.7	32.3	32.3	30.4	27.3	24.8	25.4	27.4	25.3	23.3
2012	23.6	28.1	29	32.5	30.9	29.3	25.7	24.4	25.5	27.1	27	24.3
2013	26	28.5	30.8	32.2	31.6	29.9	26.4	24.5	26	27.3	27.9	24.3
2014	24.4	26.3	30.5	31.4	31.1	30.8	27.4	24.9	25.9	27.3	27.4	24.7
2015	22.5	28.3	31.3	31.3	32.7	31	27.8	25.6	26.7	28.4	27.1	21.6
2016	22	25.7	32.5	33	31.8	29.2	26.2	25.3	26.6	28.7	28.5	25.9
2017	26.8	26.1	30.6	32.5	32.4	29.3	26.4	25.5	26.4	28.4	27.1	25.7
2018	22.1	28.9	31.1	32.4	32.6	29.2	25.9	24.8	25.8	27.7	27	24.4
2019	25	26.5	31	32.9	32.2	28.9	26.7	24.7	26	25.4	26.1	23.7
2020	22.6	25.5	30.3	32.8	32.4	30.8	26.6	24.6	25.8	27.6	26.6	25.7

Table 11. *Temperature of Pala (˚C) at 2m above the ground.*

year	Jan	Feb	Mar	Apr	May	Jun	Jul	Aug	Sep	Oct	Nov	Dec
2010	27.6	30.1	31.3	33.6	31.1	27.8	25.3	24.8	25.1	26.1	27.2	24.7
2011	24.1	29.5	30.4	32.4	30.5	28.1	26	24.4	25	26.2	26	24.2

year	Jan	Feb	Mar	Apr	May	Jun	Jul	Aug	Sep	Oct	Nov	Dec
2012	25.1	29.1	30.5	32.5	29.5	26.9	24.7	24.1	24.8	26.2	27.1	24.9
2013	26.6	29.1	32.3	32.8	29.9	27.9	25.2	24.2	25.4	27	28.3	26.1
2014	26.2	28.1	31.5	31	29.4	27.8	25.9	24.4	25	26.4	27.6	25.3
2015	24.1	29.7	32	32.3	31.8	28.7	26.2	25.2	25.7	26.7	26.7	23.1
2016	24.2	28.2	33	32.8	29.8	27.1	25.7	25.1	25.8	27.3	27.9	26.2
2017	27.3	27.5	31.8	32.3	30	27.3	25.8	25.1	25.4	27.5	27.2	26.2
2018	24	30.3	32.1	32.4	29.8	27.7	25.5	24.7	25.4	27.5	28.1	25.3
2019	26.3	28.2	32.8	33.4	30.3	26.8	25.9	24.6	25.7	25	27.4	24.5
2020	24	26.8	31.6	33.1	31.4	28.9	25.8	25.1	25.1	26.9	27.4	26.2

References

[1] Abakar Mahamat Tahir, Mahamat Adoum Abdraman, Ruben Mouangue, Alexis Kuitche, Estimate of the Wind Resource of Two Cities in the Sahara and Sahel in Chad, International Journal of Energy and Power Engineering 2020; 9(6): 86-94. https://doi.org/10.11648/j.ijepe.20200906.11

[2] Abdelhamid Issa Hassane, Abdel-Hamid Mahamat Ali, Abakar Mahamat Tahir, Jean-Marie Hauglustaine, International journal of renewable energy research Vol. 9, No. 3, September, 2019. https://doi.org/10.20508/ijrer.v9i3

[3] Dr Fatih Birol, Executive Director, International Energy Agency, Africa Energy Outlook 2022.

[4] Gour Chand Mazumder, Abu Shahadat Md. Ibrahim, Md. Habibur Rahman, Saiful Huque, Solar PV and Wind Powered Green Hydrogen Production Cost for Selected Locations, International journal of renewable energy research, vol. 11, no. 4, December, 2021. https://doi.org/10.20508/ijrer.v11i4.12516.g8327

[5] N. M. Nahar and Jagdish P. Gupta, Energy-conservation potential for solar cookers in arid zones of India, Energy Vol. 16, No. 6, pp. 965-969, 1991. https://doi.org/10.1016/0360-5442(91)90048-Q

[6] Pegah Mirzania, Joel A. Gordon, Nazmiye Balta-Ozkan, Ramazan Caner Sayan, Lochner Marais, Barriers to powering past coal: Implications for a just energy transition in South Africa, Energy Research & Social Science, Volume 101, July 2023, 103122. https://doi.org/10.1016/j.erss.2023.103122

[7] Evelyne Taryam, "Accès Énergie Tchad: Un Frein au Développement," Thinking Africa, January 2021, https://www.thinkingafrica.org/V2/lacces-a-lenergie-au-tchad-un-frein-au-developpement/

[8] Ali Ramadan Ali, Mahamat Kher Neduinga, Marinette Jeutho Gouajio, Andr é Abanda, Herv é Simo, Adoum Danao Adile, Fabien Kenmogne, Effects of adding the antiparallel diodes in a model of solar photovoltaic cell: Theory and Pspice simulations, Journal of Modern Green Energy, (2024), accepted for publication.

[9] Bali Tamegue Bernard, Donatien Njomo, Venant Sorel Chara-Dackou, Mahamat Hassane Babikir, Mahamat Ker Nediguina, Daniel Rom éo Kamta Legue, Techno-Economic Analysis of Wind Power Generation in Mongo and Abeche, Chad, International Journal of Sustainable Development and Planning, Vol. 19, No. 1, January, 2024, pp. 55-67. https://doi.org/10.18280/ijsdp.190105

[10] A. K. Azad, M. G. Rasul, T. Yusaf, (2014). Statistical Diagnosis of the Best Weibull Methods for Wind Power Assessment for Agricultural Applications. Energies, 2014, 7, 3056-3085; https://doi.org/10.3390/en7053056

[11] F. Youcef Ettoumi, A. Mefti, A. Adane, M. Y. Bouroubi, Statistical analysis of solar measurements in Algeria using beta distributions, Renewable Energy 26 (2002) 47–67. https://doi.org/10.1016/S0960-1481(01)00100-8

[12] Marinette G. Jeutho, Fabien Kenmogne and David Yem é é, Statistical estimation of mean wind energy available in western Region, of Cameroon: case of the Bafoussam's city, Journal Of Harmonized Research in Engineering 5(1), 2017, 15-27.

[13] Marinette G. Jeutho, Kenmogne Fabien, Yemele David, How to Use the Temperature Data to Find the Appropriate Site for Best Wind Speed Generation? Applications on Data Obtained from Three Different Cities of Cameroon, International Journal of Scientific Engineering and Science, Volume 2, Issue 4, pp. 53-62, 2018.

[14] Adoum Kriga, Allassem D ésir é, Andr éAbanda, Adoum Danao Adile, Yaya Dagal Dari 6 and Fabien Kenmogne, Forecast of the electrical energy demand of N'Djamena, Chad, based on the statistical method, World Journal of Advanced Research and Reviews, 2023, 17(01), 762–768. https://doi.org/10.30574/wjarr.2023.17.1.0073

[15] Lund, H. (2007). Renewable energy strategies for sustainable development. Energy 32(6). https://doi.org/10.1016/j.energy.2006.10.017

[16] Sarkar, Md. N. I. (2016) Estimation of Solar Radiation from Cloud Cover Data of Bangladesh. Renewables: Wind, Water, and Solar, 3, 11, pages 912-919. https://doi.org/10.1186/s40807-016-0031-7

[17] Ayodele, T. R. and Ogunjuyigbe, A. S. O. (2015) Prediction of Monthly Average Global Solar Radiation Based on Statistical Distribution of Clearness Index. Energy, 90, 1733-1742. https://doi.org/10.1016/j.energy.2015.06.137

[18] Liu, Y. H. and Jordan, R. C. (1960) The Inter Relationship and Characteristic Distribution of Direct, Diffuse and Total Solar Radiation from Meterological Data. Solar Energy, 4, 1-19. https://doi.org/10.1016/0038-092X(60)90062-1

[19] Jain, A., Mehta, R. and Mittal, S. K. (2011) Modeling Impact of Solar Radiation Onsite selection for Solar PV Power Plants in India. International Journal of Green Energy, 8, 486-498. https://doi.org/10.1080/15435075.2011.576293

[20] Kumar, R. and Umanand, L. (2005) Estimation of Global Radiation Using Clearness index Model for Sizing Photovoltaic System. Renew Energy, 30, 2221-2233. https://doi.org/10.1016/j.renene.2005.02.009

[21] Khorasanizadeh, H. and Mohammadi, K. (2013) Prediction of Daily Global Solar Radiation by Day of the Year in Four Cities Located in the Sunny Regions of Iran. Energy Conversion and Management, 76, 385-392. https://doi.org/10.1016/j.enconman.2013.07.073

[22] Karakoti, I., Das, P. K. and Singh, S. K. (2012) Predicting Monthly Mean Daily Diffuse Radiation for India. Applied Energy, 91, 412-425. https://doi.org/10.1016/j.apenergy.2011.10.012

[23] Hassan, G. E., Youssef, M. E., Zahraa, E., Mohamed, A. A. and Hanafy, A. A. (2016) New Temperature-Based Models for Predicting Global Solar Radiation. Applied Energy, 179, 437-450. https://doi.org/10.1016/j.apenergy.2016.07.006